INT J COMPUT COMMUN, ISSN 1841-9836
8(3):354-365, June, 2013.

Breast Cancer Diagnosis based on Spiculation Feature and Neural Network Techniques

V. Bălănică, I. Dumitrache, L. Preziosi

Victor Bălănică, Ioan Dumitrache
University Politechnica of Bucharest
Romania, 060042 Bucharest, Splaiul Independentei, 313
vicord20011@gmail.com, idumitrache@ics.pub.ro

Luigi Preziosi
University of Politechnics Torino
Italy, 10129 Torino, Corso Duca degli Abruzzi, 24
luigi.preziosi@polito.it

Abstract: The degree of spiculation of the tumor edge is a particularly relevant indicator of malignancy in the analysis of breast tumoral masses. This paper introduces four new methods for extracting the spiculation feature of a detected breast lesion on mammography by segmenting the contour of the lesion in a number of regions which are separately analysed, determining a characterizing spiculation feature set. In order to differentiate between benign and malignant tumors based on the extracted spiculation sets, an intelligent neural network is first trained on a number of 96 cases of known breast cancer malignancy and then tested for diagnosing and classifying breast cancer tumors. The input of the neural network is thus the extracted spiculation feature set and the output is represented by the histopatological diagnostic given by doctors. Finally, the performance of the introduced methods is analysed depending on the number of regions in which the contour is segmented and the performance-related conclusions are stated for each of the methods.
The highlight of this paper is the division of the tumour contour in regions and the assessment of a spiculation indicator for each region, resulting a set of spiculation indicators that characterise the tumour and - by training a neural network - can be used in classifying breast tumours with high performance.
Keywords: breast cancer, spiculation feature extraction, neural network, diagnosis.

1 Introduction

In the detection process of suspicious breast cancer lesions, mammography screening is usually followed by an analysis of diagnostic mammography, i.e. a more detailed analysis of the artifacts visible on the mammographic imaging results, such as: breast tissue density, tumoral masses, (macro- and micro-) calcifications, architectural distortion, etc, [1]. Among them, the detected microcalcifications and the identified masses (also known as tumours) are considered the most relevant signs of malignancy that need to be investigated in detail. On one hand, the microcalcifications are tiny mineral deposits within the breast, representing an early indicator of the presence of a tumor. On the other hand, the tumoral mass is a tissue composed of an abnormal growth of cells (normal or neoplastic, cancerous, cells) with or without integrated calcifications that are also being detected on the mammographic results. When analyzing any pathology of breast cancer, the location, the size, the shape of the mass are usually assessed and the mass density and the tumoral margins are moreover evaluated. While the benign masses have usually smooth edges, are well circumscribed, compact and approximately circular or elliptical (see Figure 1), malignant lesions usually have vague edges and irregular form, presenting spiculations (i.e. a radial pattern of spiculs), [2]. Thus, in analyzing the tumoral mass, in addition to the lesion size, the degree of spiculation of the tumor edge is a particularly relevant indicator of malignancy (differences visible in Figure 1).

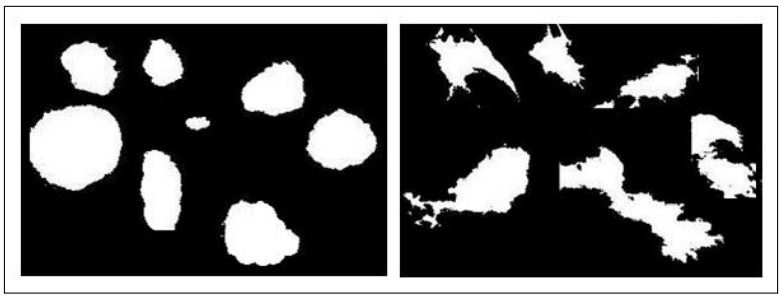

Figure 1: Benign and malignant tumors extracted from available mammographies

The evaluation of the spiculations of masses visible on the mammographic results implies form recognition techniques that extract numerical information usable in the process of differentiating between benign and malignant tumours. These techniques are continuously being developed and improved in order to make possible a more refined characterization of the particular morfological features and a higher classification performance. [3] computes a spiculation index that can classify tumours with 93% accuracy; [4] proposes three methods for morfological feature extraction and reaches 93% accuracy when classifying breast lesions; [5] explores the classification power of 6 contour algorithms on 349 masses using three popular classifiers (Bayesian Classifier, Fisher Linear Discriminant Analysis and Support Vector Machine) and shows that a big variation (14%) of the quality of the segmentation method influences only 4% of the classification performance given by the contour features.

Besides the current trend in technology and computer automation, the bioengineering interdisciplinary developments of the last years allowed the implementation of digital CAD (Computer Aided Diagnosis) aid tools to assist novice radiologists in making diagnostic and recommended treatments decisions, herewith providing a second opinion on the decision and playing the role of the second pairs of eyes in the analysis, certifying or not the quality and/or the choice. Although the computational CAD techniques used in determining a medical prognostic do not always provide the desired quality, their implementation using intelligent techniques (neural networks, fuzzy techniques, genetic algorithms and their hybrid variants) that are based on human experience and provide learning and adaptation abilities, demonstrates high performance in these kinds of tasks.

In this paper, we are trying to define new methods for extracting the spiculation feature set of a breast lesion identified on a mammographic result by analyzing the lesion contour on a number of contour regions. The methods have been tested by using a neural architecture integrated into a CAD that provides good classification performance when trained on the extracted spiculation feature sets of 96 breast cancer cases with known malignancy diagnostic. Thus, this neural CAD is able to distinguish, diagnose and classify breast cancer tumors in benign or malignant, highlighting the benefit and usefulness of both the methods and their neural CAD application in national breast cancer screening programs.

2 Materials and methods

In terms of imaging, the starry distortions visible on mammography are caused by the intrusion of cancer in surrounding tissue (invasion occurs in malignant tumors), so that the contour/outline form of the tumor is generally correlated to the degree of malignancy. The contour is thus an extremely valuable information in the differentiation between benign and malignant tumors. As stated above benign tumors usually have smooth, circumscribed, macrolobulate and well defined contours (Figure 1), while malignant tumors are characterized by vague, irregular,

microlobulate and spiculate contours (Figure 1). Based on these observations, researchers have defined certain objective and quantitative measures/indicators to characterize the contours in order to improve the imaging classification capability of the detected tumors. In terms of performance, among the most important and most frequent contour indicators found in the literature we count: the degree of compactness, the spiculation index, the fractional concavity, the Fourier factor and the fractal dimension, [6].

In our paper, the neural networks are used for classifying the tumours based on the extracted spiculation feature set of a breast lesion identified on a mammographic result. The neural networks (NNs) models are simplified structural and functional nervous systems, formed by a number of processing elements, the neurons, which are bound by weighted connections, similar to the neural synapses, [7]. The neural network architecture mainly used in the medical field is known as the multi-layer perceptron (or MLP), [8], Figure 2, which consists of neurons usually organized in three feed-forward interconnected layers (i.e. all neurons in one layer are fully connected to all neurons in the next layer, but there are no feedbacks to previous layers). A perceptron has the ability to learn, to self-organize and to generalize (i.e. it can have same output for similar sets of inputs). The most commonly algorithm used for training the neural network is the back-propagation algorithm, which calculates the error gradient of the network and adjusts each connection weight by minimizing the mean square difference and achieving convergence to a local minimum, [9]. Figure 2 shows a graphical representation of such a network, where, in the case of a medical system, the input layer neurons often corresponds to the clinical symptoms, the hidden layer simulates the medical inference process done by the doctor and the neurons from the output layer correspond to the medical diagnosis.

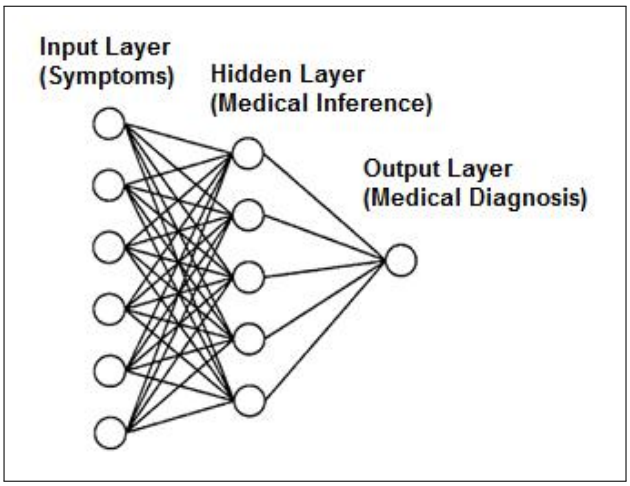

Figure 2: Graphical representation of a MPL neural network with one hidden layer

The focus in this paper is not to develop a novel MPL, but rather to apply it in the clinical relevant problem of breast cancer. Because many clinical scenarios can not be explained based on only one parameter, but as interaction of various clinical-pathological factors, [10], the inputs of the MPL may include any set of mammographic descriptors of the calcifications (distribution, number, description), of the detected masses (size, shape, density, margins, location) or of any other associated findings (asymmetries, distorsions), being able to include also inputs related to the patient history. The ouputs of the MPL are usually numbers between zero and one that may correpond to the prediction of the biopsy outcome (benign or malignant) as in [11], the stage of development for the analyzed lesion (in situ or invasive) or it may be correlated to the survival chance/rate of the patient (under 1 year, under 2 years, under 3 years, under 5 years, more than 5 years) as in [12].

3 New methods for lesion spiculation feature extraction

The mammographic lesions segmentation methods proposed below assumes that the spicules are visible on the mammography in the form of tumor infiltration or branches, usually narrow, in normal biological tissue. Therefore, the analysis of tumor contour on neighborhoods (or regions) of the contour and the measuring of the curvature change in each region offers an useful set of valuable information in determining the degree of spiculation in the analysed regions of the lesion contour and allowing subsequent CAD classification of tumors in benign or malignant.

For each of the neighborhoods of the lesion contour four spiculation indicators are computed, namely:

A. A Maximum Level Difference for every region of the contour, relative to the center of gravity of the lesion, according to the following figure (Figure 3):

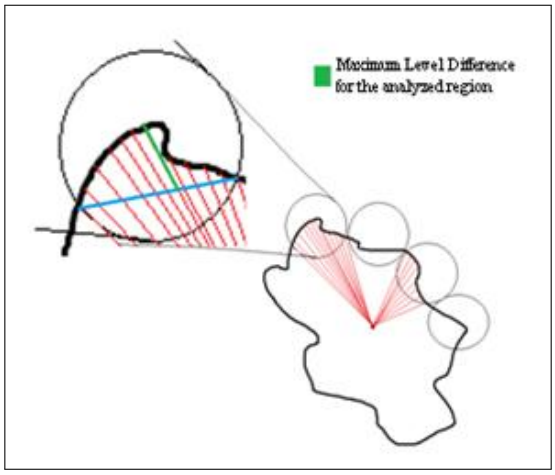

Figure 3: Calculation of the maximum level difference of for the regions of the tumoral contour

B. The Total Area of triangles in a neighborhood, calculated by adding the triangle areas formed by each three consecutive points along the contour, according to the following figure (Figure 4):

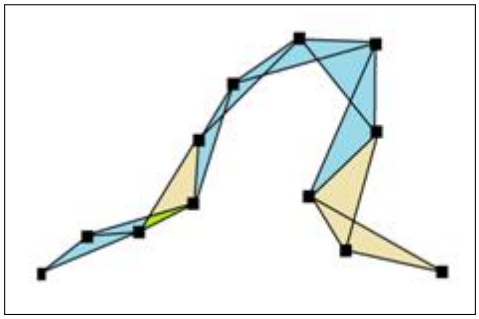

Figure 4: Calculation of the total area of the triangles formed along the contour for a contour region

C. The Total Angle in a neighborhood, calculated by adding all the angles formed by every three consecutive points along the contour, according to the following figure (Figure 5):

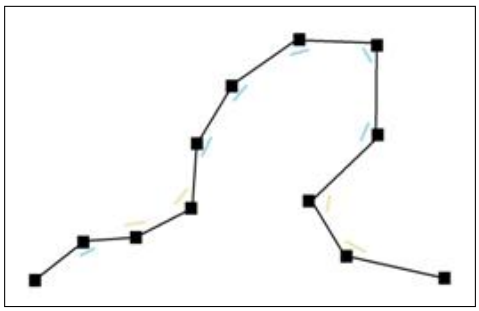

Figure 5: Calculation of total angle summed for the angles formed along a contour region

D. The Total Quadratic Curvature for each region, calculated by adding the curvatures of the circles passing through each three consecutive points along the contour, according to the following figure (Figure 6):

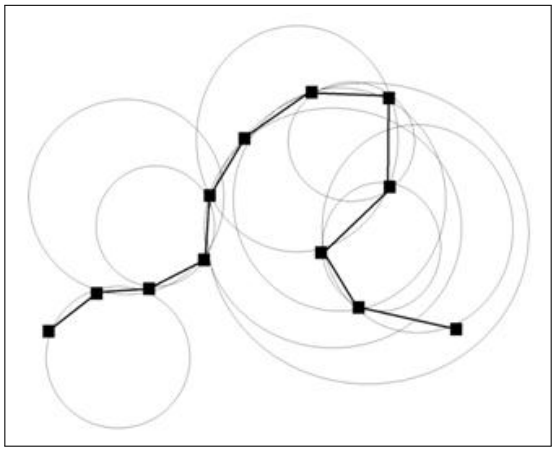

Figure 6: Calculation of the total quadratic curvature, by adding the curvatures of the circles passing through each three consecutive points of the analysed region of the contour

The main steps for the defined A, B, C and D methods are described as following:

i. The starting point of the method is an image of a detected mass (Figure 7 a),

ii. Calculate and plot the center of the mass based on the pixels that form the lesion (computing center of mass for lines and for columns) (Figure 7 b),

iii. Calculate and plot the marginal pixels of the tumor (Figure 7 b),

iv. Calculate and plot the distances between the center of mass and the pixels describing the edge of the tumor (Figure 7 c),

v. The distance vector is ascendently ordered according to the angle formed by these distances lines with one reference line,

vi. Depending on a relevant, experimentally determined, number of neighborhoods, X, for each angle Z = 360/X are done a number of operations specific for each algorithm. For each angle Z, for algorithm:

A. Is computed the maximum difference of the distances (= center of gravity - marginal pixels) that fall within the Z angle, thus identifying the characteristic vector of spiculation for the tumor. Table 1 shows an example of this vector for a malignant and a benign lesion).

B. Is computed the total area of triangles in the neighborhood described by the Z angle, by adding the areas of the triangles formed by every three consecutive points along the contour, according to the formula (1), [13]. Table 1 shows an example of this vector for a malignant and a benign lesion).

$$\sum_{i\epsilon Z} A_i, A_i = \frac{1}{2}[(X_i - X_{i+2})(Y_{i+1} - Y_i) - (X_i - X_{i+})(Y_{i+2} - Y_i)] \tag{1}$$

C. Is computed the total angle for the neighborhood described by the Z angle, by summing of all angles formed by every three consecutive points along the contour, according to the formula (2), [13]. Table 2 shows an example of this vector for a malignant and a benign lesion).

$$\sum_{i\epsilon Z} U_i, U_i = arcsin[2{\cdot}A_i/\sqrt{(X_i - X_{i+1})^2 + (Y_i - Y_{i+1})}{\cdot}\sqrt{(X_{i+1} - X_{i+2})^2 + (Y_{i+1} - Y_{i+2})}] \tag{2}$$

D. Is computed the total quadratic curvature for the neighborhood described by the Z angle, by adding quadratic curvatures of the circles passing through each three consecutive points along the contour, according to the formulas (3), (4), (5), [13]. Table 2 shows an example of this vector for a malignant and a benign lesion).

$$\sum_{i\epsilon Z} c_i, c_i = \frac{1}{R_i^2}, R_i = \sqrt{\frac{d^2 + e^2}{4a^2} - \frac{f}{a}}, where \tag{3}$$

$$a = \begin{vmatrix} X_i & Y_i & 1 \\ X_{i+1} & Y_{i+1} & 1 \\ X_{i+2} & Y_{i+2} & 1 \end{vmatrix}, d = \begin{vmatrix} X_i^2 + Y_i^2 & Y_i & 1 \\ X_{i+1}^2 + Y_{i+1}^2 & Y_{i+1} & 1 \\ X_{i+2}^2 + Y_{i+2}^2 & Y_{i+2} & 1 \end{vmatrix}, \tag{4}$$

$$e = \begin{vmatrix} X_i^2 + Y_i^2 & X_i & 1 \\ X_{i+1}^2 + Y_{i+1}^2 & X_{i+1} & 1 \\ X_{i+2}^2 + Y_{i+2}^2 & X_{i+2} & 1 \end{vmatrix}, f = \begin{vmatrix} X_i^2 + Y_i^2 & X_i & Y_i \\ X_{i+1}^2 + Y_{i+1}^2 & X_{i+1} & Y_{i+1} \\ X_{i+2}^2 + Y_{i+2}^2 & X_{i+2} & Y_{i+2} \end{vmatrix} \tag{5}$$

The spiculation features set computed with any of the four methods shows, after tests, a very good performance in terms of differentiating benign and malignant tumors and can be used to compute an objective measure/degree of spiculation for the examined lesions. Moreover, these methods are suitable for training a neural classifier of malignant or benign patterns of spicules that is able to make assessments in the presence of a new set of extracted mammographic spiculation features.

As observed, depending on the analyzed lesion, the nature of these sets of indicators show a large variation of values in each neighborhood which makes them very suitable to being analyzed with classification modules such as neural networks in order to determine patterns and nonlinear correlations. The following practical approach shows the great classification potential of these indicators, given the fact that the trained neural modules reached maximum performance after a very short training time.

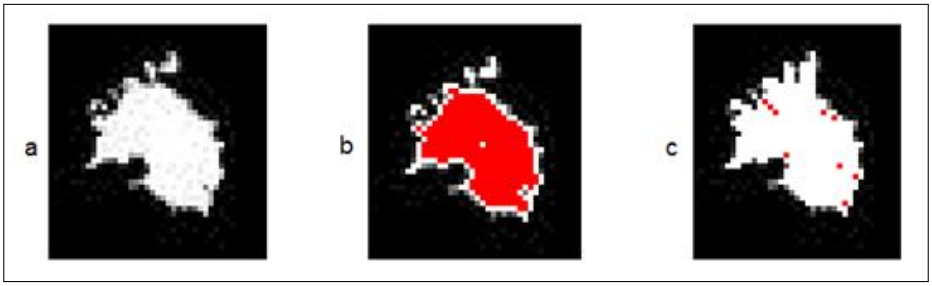

Figure 7: Lesion segmentation algorithm for computing the spiculation degree: a) a tumor identified on mammography, b) identification of the center of the mass and of the marginal pixels, c) calculating and sorting the angular distances from the center of the mass to the marginal pixels

Spiculation	Malignant	Benign
Region 1	0.029088023	0.002314645
Region 2	0.010393358	0.003456135
Region 3	0.013055199	0.010551446
Region 4	0.011486832	0.003844839
Region 5	0.012432602	0.024487918
Region 6	0.008171691	0.022505824
Region 7	0.008919256	0.004633745
Region 8	0.008129058	0.006751543
Region 9	0.004758858	0.005050591
Region 10	0.008588636	0.001135357
Region 11	0.005033413	0.023203568
Region 12	0.006881693	0.001615465
Region 13	0.012579647	0.007542353
Region 14	0.015354234	0.006765708
Region 15	0.032946416	0.005762422
Region 16	0.011897444	0.008253233
Region 17	0.00767037	0.014833624
Region 18	0.015423039	0.006765275
Region 19	0.011775156	0.002545662
Region 20	0.040558593	0.000563123

Total Area	Malignant	Benign
Region 1	-86	0
Region 2	969.5	-0.5
Region 3	26.5	-5.5
Region 4	2011	0
Region 5	2500.5	12
Region 6	2146.5	-152
Region 7	630.5	455.5
Region 8	809.5	263.5
Region 9	-1240.5	295.5
Region 10	-875	138.5
Region 11	574	-192
Region 12	2032.5	110.5
Region 13	-986.5	253
Region 14	-998	-463.5
Region 15	-925.5	3.5
Region 16	-1005.5	-12
Region 17	88.5	84.5
Region 18	-196.5	52.5
Region 19	-226	190.5
Region 20	-111.5	1

Table 1: The characteristical spiculation vectors for a malignant lesion and for a benign one for method A and method B

However, the efficient utilization of these methods may vary depending on the size and the quality of the imaging results (processed or unprocessed, noise filtered or unfiltered regions of interest, the quality of image binarization, etc.) and in what concerns the choice of the number of neighborhoods for the segmentation of the lesion contour. In this respect, one can successfully use a genetic algorithm to determine the optimal number of neighborhoods to achieve the maximum classification performance.

4 Neural networks trained for breast cancer diagnosis

The data sets obtained by applying the above methods can be used to train a neural intelligent module for the classification of the detected lesions on imaging results and determine the nonlinear correlations and the useful predictions. Thus, a feedforward neural network with one hidden layer, configurable in terms of the learning rate, of learning momentum, of the training epochs and of the minimum desired error, was trained using the backpropagation learning algorithm based on the extracted imaging spiculation feature sets determined with the above defined A, B, C and D methods (the feature sets will be noted as SetA, SetB, SetC and SetD). The

Total Angle	Malignant	Benign
Region 1	-158.9006115	10.30484647
Region 2	237.1041222	4.950272234
Region 3	170.4773613	-4.57392126
Region 4	105.8239209	0
Region 5	294.29397	-18.237718
Region 6	184.6354634	-14.2500327
Region 7	222.5665005	114.3045493
Region 8	156.3273605	57.12501634
Region 9	-169.667477	152.5138742
Region 10	-191.3721008	92.35031797
Region 11	84.80557109	-14.48976259
Region 12	362.1537249	6.441600099
Region 13	-176.3714678	152.8003632
Region 14	-66.65995455	-177.6626941
Region 15	-52.69605172	28.73979529
Region 16	-372.1805601	-1.708935032
Region 17	-48.36646066	65.11551647
Region 18	151.9275131	105.697576
Region 19	-101.3099325	86.37062227
Region 20	49.76364169	-22.87805803

Total Curvature	Malignant	Benign
Region 1	0.016552033	0.001116978
Region 2	0.019112517	0.001126586
Region 3	0.005208189	0.001130842
Region 4	0.002593499	0.001182075
Region 5	0.001063093	0.001469999
Region 6	0.001792455	0.001252206
Region 7	0.002036859	0.00123547
Region 8	0.002299495	0.001290132
Region 9	0.002999928	0.001390865
Region 10	0.002855358	0.001224238
Region 11	0.003950692	0.001623056
Region 12	0.003452697	0.001583039
Region 13	0.003150858	0.001771651
Region 14	0.004421394	0.001892085
Region 15	0.018709067	0.001960565
Region 16	0.006304613	0.002043145
Region 17	0.009259506	0.002107581
Region 18	0.008482187	0.002189537
Region 19	0.010724884	0.002172309
Region 20	0.02949604	0.002275411

Table 2: The characteristical spiculation vectors for a malignant lesion and for a benign one for method C and method D

general training and testing algorithm of the neural module is given below:

i. Having a selection of mammographies for which the diagnostic output is known, i.e. the diagnosis (benign or malignant),

ii. The spiculation set for each of the mammographies is extracted with one of the A, B, C, or D methods described above, for a number of neighborhoods,

iii. Both the input (the spiculation data set) and also the output (the diagnostic) are normalized,

iv. Based on the normalized data, the neural network is being trained and validated for the predicton of the output (the diagnostic),

v. The predicted output is compared with the actual output (truth values of malignancy) by calculating performance measures like: specificity (i.e. number of true negatives divided by the sum of true negatives and false positives), sensitivity (i.e. number of true positives divided by the sum of true positives and false negatives), accuracy (i.e. sum of true positives and true negatives divided by sum of true positives, false positives, true negatives and false negatives) and the Matthews Correlation Coefficient (MCC explained below).

The training, the testing and the validation of the neural modules are based on the information of 96 mammographic cases acquired from the Department of Medical Physics, University of FreeState, Bloemfontain, South Africa, of which 48 cases are benign and 48 are malignant, [14].

The practical experience has focused on the analysis of several selections of features in order to determine the training and classification performances of the neural networks. Rapid convergence of the training error and the classification and prediction power of the neural network indicate the correlation strength/weight between inputs and outputs, directly justifying the existence or the absence of non-linear correlations between them, in this case evaluated by Matthews Correlation Coefficient (MCC) - belonging to the interval [-1, +1], +1 representing a perfect correlation, 0 an arbitrary correlation and -1 inverse correlation.

Because the quality of the spiculation characteristics introduced in the previous section may vary depending on the number of neighborhoods set for segmentation of the lesions contour, the tests include also the variation of this value. Simultaneously, the regions of interest (ROI) processed and used in evaluating the imaging characteristics have the dimension of 335x436 pixels, an increase of the size being possible to the expense of the time needed for extracting data and for running the tests.

On average, 5 to 8 neural networks were trained for the same set of features in order to observe and determine the recorded performance variation. The performed tests (see Table 3) are not exhaustive, the results being obtained based on the currently available data sets.

5 Discussion of results

The performance results presented in Table 3 give a clear indication about the high potential of the introduced spiculation-feature extraction methods in what concerns the differentiation between benign and malignant tumors when using a neural classifier.

However, as shown in Table 4, the developed methods differ in terms of power and speed of convergence of the classifications and provide a different classification stability when changing the number of analyzed lesion contour neighborhoods. Thus, the method that calculates the maximum level difference on each region of the contour offers the optimal method for extracting the spiculation feature and the algorithm that calculates the total quadratic curvature for each region offers the most reliable measure of the lesion malignancy regardless of the neighborhoods number.

6 Conclusions

This paper introduces four new methods for the assessment of the tumor contour on a number of boundary neighborhoods. The Maximum Level Difference is calculated for every region of the analyzed contour, relative to the center of gravity of the lesion. The Total Area of Triangles in a neighborhood is calculated by adding the areas of each triangle formed by three consecutive points along the contour. The Total Angle for a neighborhood is calculated by adding up all the angles formed by every three consecutive points along the contour. The Total Quadratic Curvature for each region is calculated by adding the curvatures of the circles passing through each three consecutive points along the contour.

The spiculation feature extraction algoritms are tested on a selection of mammographies with known diagnostic by using a neural network that is trained on the extracted feature sets.

Following the performance tests, the spiculation feature sets computed with all of the four methods show a high potential in the differentiation of benign and malignant tumors and can be used to compute an objective measure/degree of spicularity for the analysed lesion. Moreover, these methods are suitable for training a neural classifier of malignant or benign patterns of spiculs that is able to make assessments in the presence of a new set of extracted mammographic spiculation features. However, as shown in the pages of the paper, the developed methods differ in terms of power and speed of convergence of the classifications and provide a different classification stability when changing the number of neighborhoods the lesion contour is segmented and analyzed.

These CAD extraction methods show high reliability and prove high implementation potential being currently used in an automated decision support systems for breast cancer designed for national mammography screening programs in Romania and South Africa.

ID	No. of neighborhoods	Inputs of the neural network	Outputs of the neural network	Malignity classification performances	MCC Correlation
1	5	SetA =5 inputs	Diagnostic	Sensitivity: [97 100 %] Specificity: [100 98.1 %] Accuracy: [98.9 %] For 50-200 training iterations	0.97
2	5	SetB =5 inputs	Diagnostic	Sensitivity: [86.3 100 %] Specificity: [96.2 83 %] Accuracy: [91.7 90.7 %] For 100-300 training iterations	0.83
3	5	SetC =5 inputs	Diagnostic	Sensitivity: [90.9 93.1 %] Specificity: [90.5 98.1 %] Accuracy: [90.7 95.8 %] For 100-300 training iterations	0.86
4	5	SetD =5 inputs	Diagnostic	Sensitivity: [97.7 100 %] Specificity: [98.1 98.1 %] Accuracy: [97.9 98.9 %] For 50-100 training iterations	0.98
5	5	The best sets: SetA,SetB =10 inputs	Diagnostic	Sensitivity: [100 %] Specificity: [100 %] Accuracy: [100 %] For 20-40 training iterations	1
6	5	SetA,SetB, SetC,SetD =20 inputs	Diagnostic	Sensitivity: [87.7 91.6 %] Specificity: [97.9 100 %] Accuracy: [92.7 95.8 %] For 100-300 training iterations	0.90
7	20	SetA =20 inputs	Diagnostic	Sensitivity: [100 %] Specificity: [100 %] Accuracy: [100 %] For 20-30 training iterations	1
8	20	SetB =20 inputs	Diagnostic	Sensitivity: [100 %] Specificity: [100 %] Accuracy: [100 %] For 50-150 training iterations	1
9	20	SetC =20 inputs	Diagnostic	Sensitivity: [100 %] Specificity: [100 %] Accuracy: [100 %] For 4-10 training iterations	1
10	20	SetD =20 inputs	Diagnostic	Sensitivity: [100 %] Specificity: [100 %] Accuracy: [100 %] For 150-200 training iterations	1
11	20	The best sets: SetA,SetC =40 inputs	Diagnostic	Sensitivity: [100 %] Specificity: [100 %] Accuracy: [100 %] For 3 training iterations	1
12	20	SetA,SetB, SetC,SetD =80 inputs	Diagnostic	Sensitivity: [100 %] Specificity: [100 %] Accuracy: [100 %] For 3-4 training iterations	1

Table 3: The trained neural networks and the achieved performances

Set ID	**Description of the Spiculations Feature Set**	**Observed features**	**Description**
SetA	Spiculation set for the A algorithm: The Maximum Level Difference for every region of the contour	Average convergence and avarage stability	Regardless of the neighborhoods number, the classification performance converges with average speed, and the obtain results vary very little.
SetB	Spiculation set for the B algorithm: The Total Area of Triangles in a neighborhood	Slow convergence and low stability	Regardless of the neighborhoods number, the classification performance converges with low speed. For a small number of regions, the results are much weaker compared with those obtained for a higher number of regions.
SetC	Spiculation set for the C algorithm: The Total Angle in a neighborhood	Fast convergence and low stability	Regardless of the number of neighborhood, the classification performance converges with high speed. For a small number of regions, the results are poor compared to those obtained for a larger number of regions.
SetD	Spiculation set for the D algorithm: The Total Quadratic Curvature for a region	Slow convergence but very high stability	Regardless of neighborhoods number, the classification performance converges with low speed, but the results are always powerful and do not vary.

Table 4: The efficiency of the spiculation feature extraction methods for a lesion

Bibliography

[1] Sultana, Alina (2010); *On Improving Image-Based Diagnosis Using Digital Image Processing*, Faculty of Electronics, Telecommunications and Information Technology, Bucharest.

[2] Feig, S.A.; Yaffe, M.J. (1995); Digital Mammography, Computer-Aided Diagnosis and Telemammography, *The Radiologic Clinics of North America*, Breast Imaging Press, 33(6):1205-1230.

[3] Guliato, D.; Rangayyan, R.M.; Carvalho, J.D.; Santiago, S.A. (2006); Spiculation-preserving Polygonal Modeling of Contours of Breast Tumors, *Proceedings of the 28th IEEE*, 2791-2794.

[4] Cheikhrouhou, I.; Djemal, K.; Sellami, D.; Maaref, H.; Derbel, N. (2008); New mass description in mammographies, *Image Processing Theory, Tools and Applications.*

[5] DomĂnguez, A.R.; Nandi, A.K. (2009); Toward breast cancer diagnosis based on automated segmentation of masses in mammograms, *Pattern Recognition*, 42(6):1138-1148.

[6] Rangayyan, R.M.; Nguyen, T.M. (2005); Pattern classification of breast masses via fractal analysis of their conturs, *International Congress Series*, 1281:1041-1046.

[7] Dumitrache, I.; Buiu, C. (1995); Hybrid geno-fuzzy controllers, *IEEE Intelligent Systems for the 21st Century*, 5:2034-2039.

[8] Pandey, B; Mishra, R.B. (2009); Knowledge and intelligent computing system in medicine, *Computers in Biology and Medicine*, 39:215-230.

[9] Alpaydin, Ethem (2010); Introduction to machine learning, *MIT Press*, 2010.

[10] Drew, P. J.; Monson, J. R.T. (2000); Artificial neural networks, *Surgery*, 127:3-11.

[11] Marcano-Cedeno, A.; Quintanilla-Dominguez, J.; Andina, D. (2011); Breast cancer classification applying artificial metaplasticity algorithm, *Neurocomputing*, 74:1243-1250.

[12] Mofidi, R.; Deans, C.; Duff, M.D.; Beaux, A.C.; Brown, S. P. (2006); Prediction of survival from carcinoma of oesophagus and oesophago-gastric junction following surgical resection using an artificial neural network, *European Journal of Surgical Oncology*, 533-539.

[13] Hazewinkel, M. (1994); *Encyclopaedia of Mathematics* (set), Kluwer, ISBN 1-55608-010-7.

[14] Balanica, V.; Rae, W.I.D.; Caramihai, M.; Acho, S.; Herbst, C.P. (2009); Integration of image and patient data, software and international coding systems for use in a mammography research project, *World Academy of Science, Engineering and Technology*, 58:1002-1005.